

Improving the Stability of Mesoporous MCM-41 Silica via Thicker More Highly Condensed Pore Walls

Robert Mokaya[†]

Department of Chemistry, University of Cambridge, Lensfield Road, Cambridge CB2 1EW, U.K.

Received: June 29, 1999; In Final Form: September 10, 1999

Thicker-walled mesoporous MCM-41 silicas with improved thermal and hydrothermal stability were prepared via secondary crystallization (in which calcined MCM-41 was used as silica source) or by using long crystallization times. Unusually, the thicker pore walls of the as-synthesized (surfactant containing) forms of these Si-MCM-41 materials are primarily made up of fully condensed silica units. Q^4/Q^3 ratios as high as 3.4 or 4.5 are obtained for two-step (48 h each) crystallization or 96 h crystallization at 150 °C, respectively. A diffusion-controlled mechanism in which silicate units and surfactant molecules are continually added onto the “seed” crystals (during secondary recrystallization) or to the growing surfactant/silicate aggregate (for long crystallization time) is proposed to explain the pore wall thickening and higher silica condensation.

Introduction

The thermal and hydrothermal stability of purely siliceous MCM-41 (Si-MCM-41) silicas has been a recurring research theme since their discovery. The thermal stability of Si-MCM-41 is relatively good, and the materials have been shown to be stable at temperatures of up to 850 °C.¹ They are nevertheless usually destroyed, and their surface area is reduced to virtually nil on calcination at 1000 °C.² Their hydrothermal stability, especially in boiling water, is also very poor. Indeed, when subjected to refluxing in water for short periods of time, conventional Si-MCM-41 materials readily lose their hexagonal structure and are rendered amorphous.³ This lack of hydrothermal stability is a considerable drawback with respect to the use of Si-MCM-41 in applications requiring the presence of water such as in ion exchange and catalysis. Recently, new varieties of silica mesostructures with unique morphologies that exhibit greater hydrothermal stability have been synthesized.^{4–6} A major difference between Si-MCM-41 and such mesostructures is that they either possess much thicker pore walls (e.g., SBA-15)⁴ and therefore a high pore wall pore size aspect ratio or are less well ordered (e.g., KIT-1 and MSU-G).^{5,6}

The pore wall thickness of Si-MCM-41 may be controlled by careful choice of synthesis conditions^{7,8} or by postsynthesis restructuring.^{9,10} The stability of Si-MCM-41 may also be improved via postsynthesis hydrothermal restructuring of the as-synthesized (surfactant containing) material in water¹¹ or by addition of tetraalkylammonium or inorganic salts to the synthesis gel.^{12,13} However, as yet there have been no reports on any systematic preparation and assessment of the thermal and hydrothermal stability of Si-MCM-41 with increasing pore wall thickness and level of silica condensation within the pore walls. Furthermore, it is not clear what role is played by pore wall thickness or extent of silica condensation as opposed to morphology in determining the stability of MCM-41 and other mesoporous silicas. With regard to the formation of a strengthened silica framework, there is at present no clear understanding of the underlying fortification mechanisms. In particular, the

processes via which pore wall thickening or higher silica condensation occur are not clearly understood. A clear understanding of these processes would enable the design of simple procedures for the preparation of Si-MCM-41 materials with improved stability. Here the preparation and stability (thermal and hydrothermal) of Si-MCM-41 possessing pore walls of varying thickness is reported. Two synthetic methods are employed to increase pore wall thickness, i.e., longer crystallization time or a two-step synthetic method in which calcined Si-MCM-41 is utilized as “silica source” and “seeds” for secondary synthesis.¹⁴ It is shown that it is possible, by simply increasing the pore wall thickness and extent of silica condensation, to prepare Si-MCM-41 with improved stability which is comparable to that of mesoporous silicas with benchmark stability.^{4–6} This report therefore illustrates the importance of the nature of the silica framework (as opposed to morphology)^{5,6} in determining the stability of mesoporous silicas and challenges the hitherto accepted view that MCM-41 silicas are inherently unstable in hot aqueous solutions. A mechanism for pore wall thickening and enhanced silica condensation is proposed and discussed.

Materials and Methods

Materials. The standard Si-MCM-41 (herein referred to as primary MCM-41) was prepared using a normal procedure¹⁴ in which tetramethylammonium hydroxide (TMAOH) and cetyltrimethylammonium bromide (CTAB) were dissolved in distilled water by stirring at 35 °C. The silica source, fumed silica (sigma), was added to the solution under stirring for 1 h. After further stirring for 1 h the resulting synthesis gel of composition $\text{SiO}_2:0.25 \text{ CTAB}:0.2 \text{ TMAOH}:40 \text{ H}_2\text{O}$ was left to age for 20 h at room temperature following which the gel was transferred to a Teflon-lined autoclave and heated at 150 °C for 48 h. The solid product was obtained by filtration, washed with distilled water, dried in air at room temperature, and calcined in air at 550 °C for 8 h. To prepare thicker-walled materials, either (i) the crystallization time (at 150 °C) was increased from 48 to 96 h—the resulting material was designated MCM-41-(96)—or (ii) a two-step procedure incorporating secondary synthesis was performed. For secondary synthesis a synthesis gel

[†] Telephone 01223-33 64 65; FAX 01223-33 63 62; e-mail rm140@cus.cam.ac.uk.

of composition similar to that used for primary synthesis was assembled except that the calcined primary MCM-41 was used as "silica source" instead of fumed silica. The experimental conditions and procedures were exactly the same as described above for the primary synthesis. The resulting material was designated as secondary MCM-41.

To assess stability, the Si-MCM-41 materials were either refluxed in distilled water (at a water-to-sample ratio of 1 L/g) for various lengths of time and dried at 130 °C prior to further characterization or calcined in air at 1000 °C for 4 h.

Characterization. Powder X-ray diffraction (XRD) patterns were recorded using a Philips 1710 powder diffractometer with Cu K α radiation (40 kV, 40 mA), 0.02° step size, and 1 s step time. Thermogravimetric analysis (TGA) was performed using a Polymer Laboratories TG 1500 analyzer with a heating rate of 20 °C/min under nitrogen flow of 25 mL/min. ^{29}Si (MAS) NMR spectra were acquired using a Chemagnetics CMX-400 spectrometer and 7.5 mm zirconia rotors at 79.4 MHz with 60° pulses and 500 s recycle delays. Chemical shifts are given as ppm from external tetramethylsilane (TMS).

Textural properties (surface area and pore volume) were determined at -196 °C using nitrogen in a conventional volumetric technique by a Coulter SA3100 sorptometer. Before analysis the previously calcined samples were oven dried at 130 °C and evacuated overnight at 200 °C under vacuum. The surface area was calculated using the BET method based on adsorption data in the partial pressure (P/P_0) range 0.05–0.2, and the pore volume was determined from the amount of N_2 adsorbed at a $P/P_0 = \text{ca. } 0.99$. The Barrett–Joyner–Halenda (BJH) method and t -plot analysis were used to determine the primary (or framework confined) mesopore surface area (S_p) and pore volume (V_p). The calculation of pore size was performed using various methods. The BJH method was used for both the adsorption and desorption branches of the sorption isotherms. Because of the near or total absence of microporosity, a simple relation based on the primary mesopore pore volume and surface area where the average primary pore size (APD_p) is given by the equation $\text{APD}_p = 4V_p/S_p$ was also used. The APD_p was also calculated on the basis of a geometric model detailed elsewhere,^{15,16} according to the equation $\text{APD}_p = cd(\rho V_p/1 + \rho V_p)^{1/2}$, where $c = 1.213$, ρ (density of silica walls) = 1.6 g/cm³,¹⁷ and d is basal spacing (d_{100}).

Results and Discussion

The N_2 sorption isotherms for the primary MCM-41, secondary MCM-41, and MCM-41(96) are shown in Figure 1. All the samples exhibit isotherms with a well-developed step in the relative pressure (P/P_0) range 0.35–0.5 characteristic of capillary condensation (filling) into uniform mesopores. The isotherms therefore indicate that all the samples possess good structural ordering and a narrow pore size distribution. The isotherms also indicate that any structural changes resulting from secondary crystallization or longer synthesis time are not necessarily at the expense of pore uniformity. Furthermore, the isotherms suggest that secondary crystallization results in a slight shift to lower pore size (pore filling step at lower P/P_0) while longer synthesis time increases the pore size. The isotherm of sample MCM-41(96) exhibits some hysteresis which is characteristic of MCM-41 materials with pores larger than 40 Å.¹⁶ The powder X-ray diffraction (XRD) patterns for the Si-MCM-41 materials before and after various thermal or hydrothermal treatments are shown in Figure 2, and Table 1 shows the corresponding textural parameters. The XRD pattern of the primary MCM-41 (Figure 1a) is typical of a well-ordered material and shows an intense

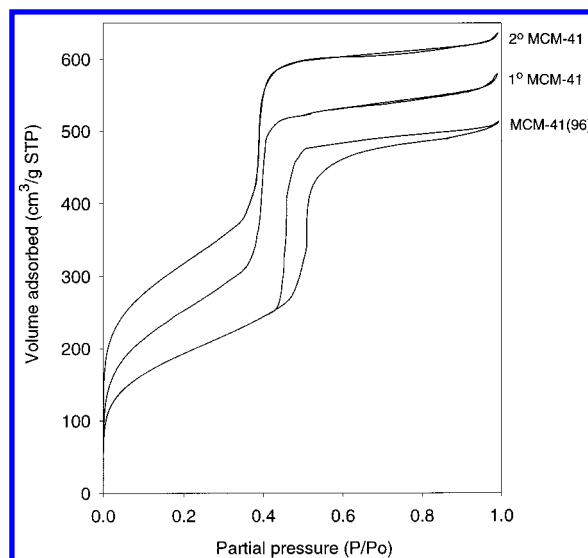


Figure 1. Nitrogen sorption isotherms of primary (1°) MCM-41, secondary (2°) MCM-41, and MCM-41(96). For clarity the isotherm of 2° MCM-41 is offset (y-axis) by 50.

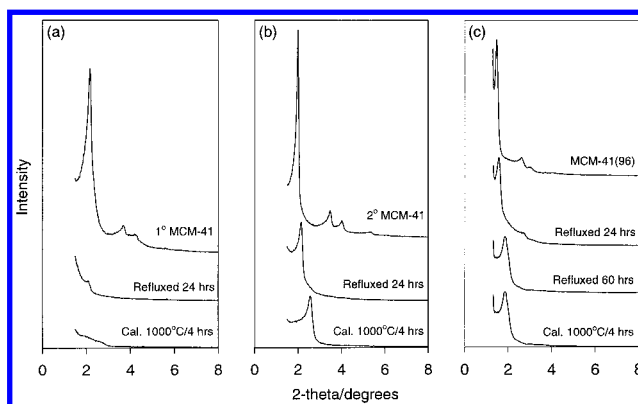


Figure 2. Powder XRD patterns of (a) primary MCM-41, (b) secondary MCM-41, and (c) MCM-41(96) before and after various thermal and hydrothermal treatments.

TABLE 1: Textural Properties of the Study Materials^a

sample	d_{100} (Å)	surf. area (m ² /g)	pore vol (cm ³ /g)	a_0^b (Å)	Q^4/Q^3
primary MCM-41	42.8	918 (880)	0.89 (0.87)	49.4	1.4
refluxed 24 h		201	0.41		
calcined 1000 °C		79	0.13		
secondary MCM-41	44.6	820 (754)	0.81 (0.72)	51.5	3.4
refluxed 24 h	41.6	705	0.92		
calcined 1000 °C	34.7	649	0.39		
MCM-41(96)	60.0	700 (624)	0.79 (0.74)	69.3	4.5
refluxed 24 h	54.5	668	0.87		
refluxed 60 h	53.2	568	0.75		
calcined 1000 °C	47.5	501	0.43		

^a Values in parentheses are primary mesopore surface area and pore volume. ^b a_0 = the lattice parameter, from the XRD data using the formula $a_0 = 2d_{100}/\sqrt{3}$.

(100) diffraction peak and some higher order peaks. Secondary synthesis (Figure 1b) results in an increase in the intensity of the (100) peak which along with an increase in intensity and improvement in the resolution of the higher order peaks indicates better long-range ordering. Sample MCM-41(96) synthesized for 96 h (Figure 1c) exhibits a (100) peak of lower intensity (compared to the secondary MCM-41) which taken together with the lower intensity of its higher order peaks may be an indication of a lower level of long-range ordering. The d_{100} data in Table

TABLE 2: Comparison of Average Pore Diameter (APD) and Corresponding Pore Wall Thickness (WT)^a Obtained by Various Calculation Methods

sample	pore diameter (Å)				wall thickness (Å)			
	BJH _{des}	BJH _{ads}	4V _p /S _p ^b	APD _p ^c	BJH _{des}	BJH _{ads}	4V/S ^b	WT _p ^c
primary MCM-41	33.4	38.7	39.1	39.6	16.0	10.7	10.3	9.8
secondary MCM-41	31.4	36.4	38.2	39.5	20.1	15.1	13.3	12.0
MCM-41(96)	38.6	46.6	47.4	53.6	30.7	22.7	21.9	15.7

^a Wall thickness = a_0 - APD. ^b Primary mesopore volume and surface area (see Table 1) were used as V_p and S_p , respectively. ^c APD_p and WT_p calculated based on a geometric model;^{15,16} 1.6 g/cm³ was used as density of the silica pore walls.¹⁷

1 show a modest increase in the basal spacing and lattice parameter (a_0) due to secondary synthesis and much larger increases for 96 h synthesis which is in agreement with previous reports.^{8–10}

Of particular relevance to the present study is the pore wall thickness of the Si-MCM-41 materials; the average pore diameter and pore wall thickness calculated using various methods are given in Table 2. In agreement with previous reports, the calculation of pore size by applying the BJH model to the desorption data underestimates the pore size with the consequence that the implied wall thickness is too high.¹⁵ It also appears that the use of the equation based on a geometric model for an infinite structure of uniform cylindrical pores arranged in an hexagonal pattern overestimates the pore size, slightly for primary and secondary MCM-41 and significantly for MCM-41(96).¹⁵ The pore sizes obtained using either the BJH model applied to adsorption data or the primary mesopore surface area and pore volume (i.e., $4V_p/S_p$) are in good agreement with each other and with the N₂ sorption isotherms and may be taken as a closer representation of the actual pore sizes. However, it is important to note that, whatever method is used, the decrease in pore size due to secondary crystallization and increase in pore size as a result of longer crystallization are clearly demonstrated. The changes in wall thickness are also consistent regardless of the method used to calculate pore size, and it is therefore reasonable to conclude from the data in Table 2 that an ~40% increase in wall thickness occurs due to secondary synthesis while synthesis at 96 h results in a 2-fold increase in wall thickness. Further evidence for the increase in wall thickness was obtained from thermogravimetric analysis of the as-synthesized (surfactant containing) samples. The ratio between the occluded template (weight loss between 120 and 350 °C) and residual silica weight (at 1000 °C) is known to vary with the wall thickness.¹⁸ Expressed as a CTMA/SiO₂ molar ratio, the calculated ratios were 0.17, 0.13, and 0.084 for primary MCM-41, secondary MCM-41, and MCM-41(96), respectively. These ratios imply that secondary MCM-41 and MCM-41(96) contain less template per unit weight of as-synthesized material. Since the variations in pore size and pore volume are only modest, it is likely that the lower CTMA/SiO₂ ratios for the secondary MCM-41 and MCM-41(96) are due to thicker pore walls. It is worth noting that the increase in wall thickness reported here (which was also observed by HRTEM) is in agreement with previous studies.^{8,10} As expected, the thicker walls of secondary MCM-41 and MCM-41(96) result in proportionately lower surface area and pore volume (see Table 1). The thicker walls reported here were also accompanied by greater silica condensation; ²⁹Si MAS NMR of the as-synthesized samples revealed a much higher proportion of fully condensed (Q⁴) silica units for the secondary MCM-41 and MCM-41(96) compared to the primary MCM-41 (see Qⁿ ratios in Table 1 and Figure 3).

The XRD patterns in Figure 1a indicate that the pore structure of the relatively thin-walled primary MCM-41 is virtually destroyed after refluxing in water for 24 h. This is reflected by

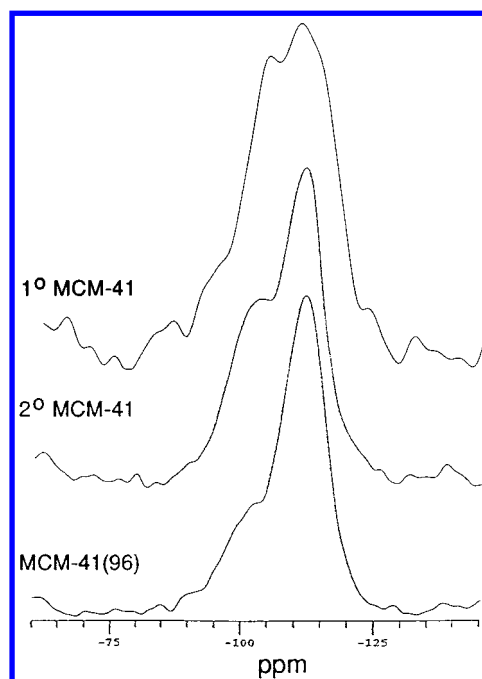


Figure 3. ²⁹Si MAS NMR spectra of as-synthesized primary (1°) MCM-41, secondary (2°) MCM-41, and MCM-41(96).

the reduction in surface area and pore volume by 80% and 45%, respectively; see Table 1. When subjected to similar hydrothermal treatment, the thicker-walled secondary MCM-41 and MCM-41(96) are able to retain structural ordering (Figure 1b,c). The retention of structural integrity in the thicker-walled materials, after being refluxed for 24 h, is confirmed by the observation that they show only a modest decrease in surface area, and their pore volumes actually increase which is probably due to a thinning of the pore walls; indeed, a rough estimate (based on a geometric model)^{15,16} of the wall thickness of secondary MCM-41 and MCM-41(96) refluxed for 24 h yielded values of 9.7 and 12.8 Å, respectively, compared to 12.0 and 15.7 Å for the starting materials. On calcination at 1000 °C for 4 h the primary MCM-41 is totally destroyed and suffers an ~90% decrease in both surface area and pore volume. Remarkably, the secondary MCM-41 and MCM-41(96) still retain some structural ordering even after calcination at 1000 °C.

The changes in the mesoporous structure (as indicated by sorption isotherms) as a result of the thermal and hydrothermal treatments are shown in Figure 4 for sample MCM-41(96). Refluxing for 24 h shifts the pore size slightly to larger values with little effect on pore size uniformity. As mentioned above, the increase in pore size is probably a result of pore wall thinning (due to dissolution of part of the pore wall) and is in agreement with the observed increase in pore volume from 0.79 to 0.87 cm³/g. Increasing the refluxing time to 60 h broadens the pore size distribution more markedly but does not destroy the framework confined mesoporosity. Calcination at 1000 °C has a much more marked effect on the mesoporous structure, and

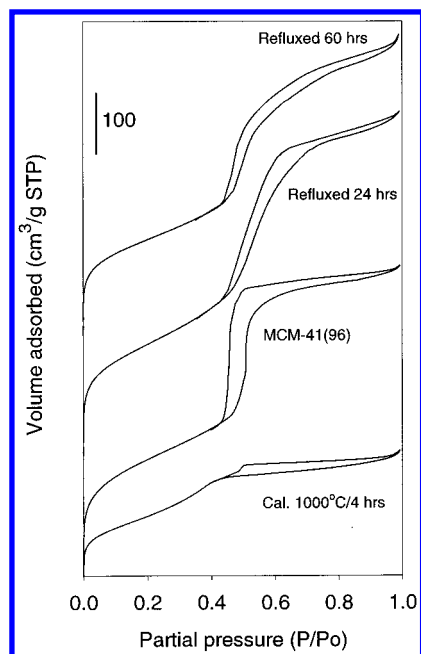


Figure 4. Nitrogen sorption isotherms of MCM-41(96) before and after various thermal and hydrothermal treatments.

it appears that the framework confined porosity, though still present, is sharply reduced with a concomitant reduction in pore size. The thermal and hydrothermal stability observed for secondary MCM-41 and especially for MCM-41(96) is unusual for pure silica MCM-41 materials which have not been modified by addition of salts to their synthesis gels during preparation.^{12,13} It is likely that the materials reported here benefit from two stabilizing effects: thicker pore walls and higher silica condensation. The influence of these factors is further illustrated by the fact that refluxing the secondary MCM-41 for 60 h resulted in a 70% decrease in surface area from 820 to 245 m²/g as opposed to a decrease of only 19% from 700 to 568 m²/g for MCM-41(96), which has thicker and more condensed pore walls; see Table 1.

Apart from thicker pore walls, another critical factor in increasing the stability of Si-MCM-41 is greater silica condensation in the pore walls.¹³ The higher level of silica condensation in secondary MCM-41 and MCM-41(96) is clearly illustrated in Figure 3, which shows the ²⁹Si MAS NMR spectra of the as-synthesized (surfactant containing) samples. The primary MCM-41 had a spectra typical of normal MCM-41 and a Q⁴/Q³ ratio of 1.4 and Q⁴/Q³ + Q² ratio of 1.1. The much higher Q⁴/Q³ ratios for secondary MCM-41 and MCM-41(96), i.e., 3.4 and 4.5, respectively, indicate that even prior to calcination the pore walls of these samples are primarily made up of fully condensed Q⁴ silica units with a small contribution from incompletely cross-linked Q³ units and hardly any Q² units. A diffusion-controlled pore channel formation mechanism¹⁹ may be invoked to explain the pore wall thickening and higher silica condensation obtained from recrystallization (secondary synthesis) or longer synthesis time. In the mechanism it is envisaged that during crystallization additional silicate units access the assembling surfactant/silicate aggregate (or silica channels for recrystallization) via the surface perpendicular to the pore axis while surfactant molecules enter along the axis.¹⁹ For secondary synthesis, silicate units may also enter the pores of the "seed" primary MCM-41 crystallites, thereby increasing both the thickness of the pore walls and the proportion of Q⁴ silica units via further condensation in a process similar to silylation. Silicate units also interact with the additional surfactant molecules on

the outer surface of the "seed" crystals forming new surfactant/silica aggregates which extend growth in the *ab* plane. The new surfactant/silica aggregates may also act as linkages between primary MCM-41 crystallites, thereby forming larger crystallites.¹⁴ Furthermore, while it is unlikely that the surfactant molecules will enter the pores of the "seed" crystals, they may however interact with silicate units at the pore mouth to extend growth in the *c*-direction. This would result in all-round crystal growth (with the crystallites of the primary MCM-41 acting as "seeds") and thus better long-range ordering (see Figure 2) and thicker pore walls but with no significant change in lattice parameter (*a*₀) since the wall thickness increases within the confines of the existing primary MCM-41 pores. This explanation is consistent with the XRD results in Figure 1 and the *a*₀ data in Table 1. On the other hand, increasing the synthesis time (from 48 to 96 h) allows for more extensive diffusion of additional silicate units and surfactant molecules into the growing surfactant/silica aggregate; additional silicate units increase the wall thickness and extent of silica condensation while additional surfactant molecules increase the density of the surfactant phase which translates to larger lattice parameter and pore size.

Another factor that may play an important role is the nature of the source of silica. The effect of different silica sources on the quality of MCM-41 products has been previously observed;²⁰ when Cab-O-sil silica and Sigma fumed silica were compared under the same preparation conditions, the latter resulted in a better ordered MCM-41 material.²⁰ In the present study the use of Cab-O-sil silica as source of silica (under similar synthesis conditions) resulted in poorer quality materials with comparatively thinner and less condensed pore walls. Using ²⁹Si (MAS) NMR, it has previously been shown that, compared to Cab-O-sil silica, fumed silica has a lower proportion of Q⁴ units, corresponding to a lower degree of silica polymerization and presumably (on dissolution) smaller silicate units. On the basis of the proposed diffusion-controlled mechanism, one might expect the nature of the silicate units (i.e., different size/mass) to influence their rates of diffusion through the growing surfactant/silica aggregate. Consequently, the less polymerized fumed silica may have silicate units with higher diffusion rates both in solution and inside the aggregate, resulting in more efficient formation of thicker walls. Further work to fully clarify the effect of the silica source is currently underway.

Conclusions

This report demonstrates that it is possible to prepare purely siliceous MCM-41 materials with improved thermal and hydrothermal stability via a one- or two-step synthesis procedure which does not involve the addition of "stabilizing salts". Improvement in stability is achieved via increase in the pore wall thickness and extent of silica condensation within the pore wall. In the one-step synthesis procedure, which simply involves increasing the time allowed for hydrothermal crystallization, pore wall strengthening into a thicker more condensed silica framework is thought to occur as a result of more extensive addition of silicate units to the growing surfactant/silica aggregates via a diffusion-controlled process. Extensive accretion of silicate units from solution encourages silica polymerization, thus increasing the wall thickness and extent of silica condensation. At the same time additional surfactant molecules access the silica-coated surfactant (micellar) phase which results in a larger basal spacing, lattice parameter, and pore size. In the two-step synthetic procedure which utilizes calcined (primary) MCM-41 as "silica source" pore wall thickening occurs when

silicate units diffuse into the pores of the primary MCM-41 crystallites, thereby increasing both the thickness of the pore walls and the proportion of Q⁴ silica units via further condensation in a process similar to silylation. The primary MCM-41 crystallites act as a "seed" for further growth, and the real source of silicate units is amorphous silica which is present in significant amounts in primary MCM-41. In the two-step procedure no significant change in basal spacing and lattice parameter occurs since the wall thickness increases within the confines of the existing primary MCM-41 pores.

Acknowledgment. The author acknowledges the EPSRC for an Advanced Fellowship.

References and Notes

- (1) Chen, C. Y.; Li, H.-X.; Davis, M. E. *Microporous Mater.* **1993**, *2*, 17.
- (2) Kim, J. M.; Kwak, J. H.; Jun, S.; Ryoo, R. *J. Phys. Chem.* **1995**, *99*, 16742.
- (3) Kim, J. M.; Ryoo, R. *Bull. Korean Chem. Soc.* **1996**, *17*, 66.
- (4) Zhao, D.; Feng, J.; Huo, Q.; Melosh, N.; Fredrickson, G. H.; Chmelka, B. F.; Stucky, G. D. *Science* **1998**, *279*, 548.
- (5) Ryoo, R.; Kim, J. M.; Ko, C. H.; Shin, C. H. *J. Phys. Chem.* **1996**, *100*, 17718.
- (6) Kim, S. S.; Zhang, W.; Pinnavaia, T. J. *Science* **1998**, *282*, 1302.
- (7) Coustel, N.; Renzo, F. D.; Fajula, F. *J. Chem. Soc., Chem. Commun.* **1994**, 967.
- (8) Cheng, C.-F.; Zhou, W.; Klinowski, J. *Chem. Phys. Lett.* **1996**, *263*, 247.
- (9) Khushalani, D.; Kuperman, A.; Ozin, G. A.; Tanaka, K.; Garces, J.; Olken, M. M.; Coombs, N. *Adv. Mater.* **1995**, *7*, 842.
- (10) Sayari, A.; Liu, P.; Kruk, M.; Jaroniec, M. *Chem. Mater.* **1997**, *9*, 2499.
- (11) Chen, L.; Horiuchi, T.; Mori, T.; Maeda, K. *J. Phys. Chem. B* **1999**, *103*, 1216.
- (12) Das, D.; Tsai, C. M.; Cheng, S. *Chem. Commun.* **1999**, 473.
- (13) Ryoo, R.; Jun, S. *J. Phys. Chem. B* **1997**, *101*, 317.
- (14) Mokaya, R.; Zhou, W.; Jones, W. *Chem. Commun.* **1999**, 51.
- (15) Kruk, M.; Jaroniec, M.; Sayari, A. *J. Phys. Chem. B* **1997**, *101*, 583.
- (16) Kruk, M.; Jaroniec, M.; Sayari, A. *Langmuir* **1997**, *13*, 6267.
- (17) Floquet, N.; Coulomb, J. P.; Goglio, S.; Grillet, Y.; Llewellyn, P. L. *Stud. Surf. Sci. Catal.* **1998**, *117*, 583.
- (18) Renzo, F. D.; Coustel, N.; Mendiboure, M.; Cambon, H.; Fajula, F. *Stud. Surf. Sci. Catal.* **1997**, *105*, 69.
- (19) Zhou, W.; Klinowski, J. *Chem. Phys. Lett.* **1998**, *292*, 207.
- (20) Cheng, C.-F.; Park, D. H.; Klinowski, J. *J. Chem. Soc., Faraday Trans.* **1997**, *93*, 193.